Supplementary Information of "Symmetry-protected four double-Weyl fermions and their topological phase transitions in nonmagnetic crystals"

Yun-Yun Bai*, Ke-Xin Pang*, and Yan Gao†

State Key Laboratory of Metastable Materials Science and Technology & Hebei Key Laboratory of Microstructural Material Physics, School of Science, Yanshan University, Qinhuangdao 066004, China

*These authors contributed equally to this work.
†Corresponding author: yangao9419@ysu.edu.cn

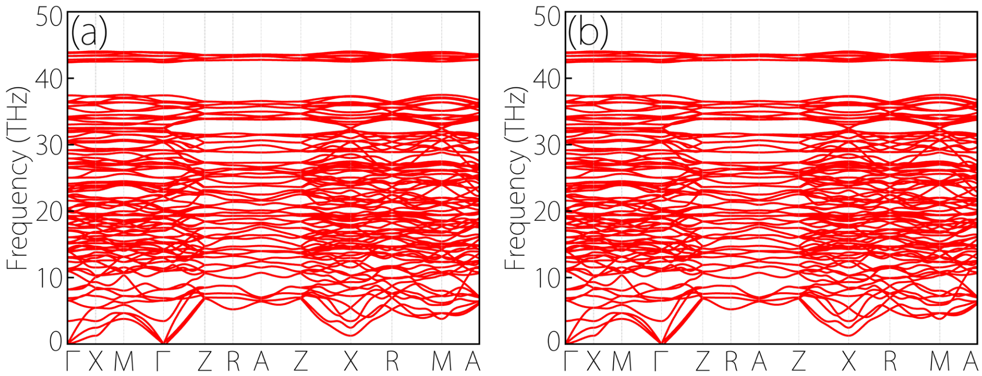

Supplementary Figure S1 | Phonon dispersion spectra. Calculated phonon band structure of (a) *l*-THRLN-C_{32} and (b) *r*-THRLN-C_{32} along the complete high-symmetry paths of the Brillouin zone. The absence of imaginary frequencies confirms the dynamical stability of THRLN-C_{32}.

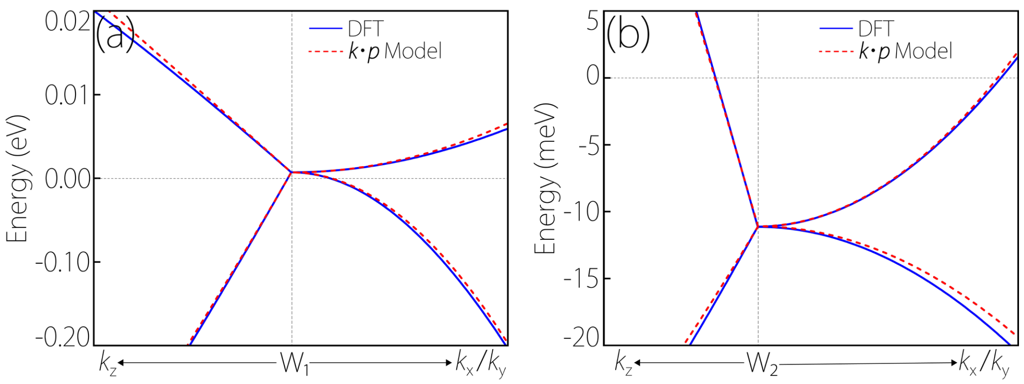

Supplementary Figure S2 | The $\boldsymbol{k}\cdot\boldsymbol{p}$ effective Hamiltonian band versus the DFT band structures for *r*-THRLN-C_{32}. a, Band dispersion along k_z and k_x/k_y at W_1 from DFT calculations (blue solid lines) and $\boldsymbol{k}\cdot\boldsymbol{p}$ model fitting (red dashed lines). Parameters for the $\boldsymbol{k}\cdot\boldsymbol{p}$ effective Hamiltonian: $\epsilon_0 = 0.82$ meV, $\epsilon_1 = 0.21\ \mathrm{eV\cdot Å}$, $\epsilon_2 = -2.75\ \mathrm{eV\cdot Å^2}$, $\epsilon_3 = 0.59\ \mathrm{eV\cdot Å^2}$, $\delta_1 = -0.66\ \mathrm{eV\cdot Å}$, $\delta_2 = 4.83\ \mathrm{eV\cdot Å^2}$, $\delta_3 = -0.74\ \mathrm{eV\cdot Å^2}$, $\alpha = 1.42 + 1.72i\ \mathrm{eV\cdot Å^2}$, $\beta = -2.12 - 2.56i\ \mathrm{eV\cdot Å^2}$. **b**, Band dispersion along k_z and k_x/k_y at W_2 from DFT calculations (blue solid lines) and $\boldsymbol{k}\cdot\boldsymbol{p}$ model fitting (red dashed lines). Parameters for the $\boldsymbol{k}\cdot\boldsymbol{p}$ effective Hamiltonian: $\epsilon_0 = -11.35$ meV, $\epsilon_1 = -0.34\ \mathrm{eV\cdot Å}$, $\epsilon_2 = 0.90\ \mathrm{eV\cdot Å^2}$, $\epsilon_3 = 0.52\ \mathrm{eV\cdot Å^2}$, $\delta_1 = 0.97\ \mathrm{eV\cdot Å}$, $\delta_2 = 3.85\ \mathrm{eV\cdot Å^2}$, $\delta_3 = 1.77\ \mathrm{eV\cdot Å^2}$, $\alpha = 0.18 + 0.10i\ \mathrm{eV\cdot Å^2}$, $\beta = -1.20 - 0.66i\ \mathrm{eV\cdot Å^2}$.

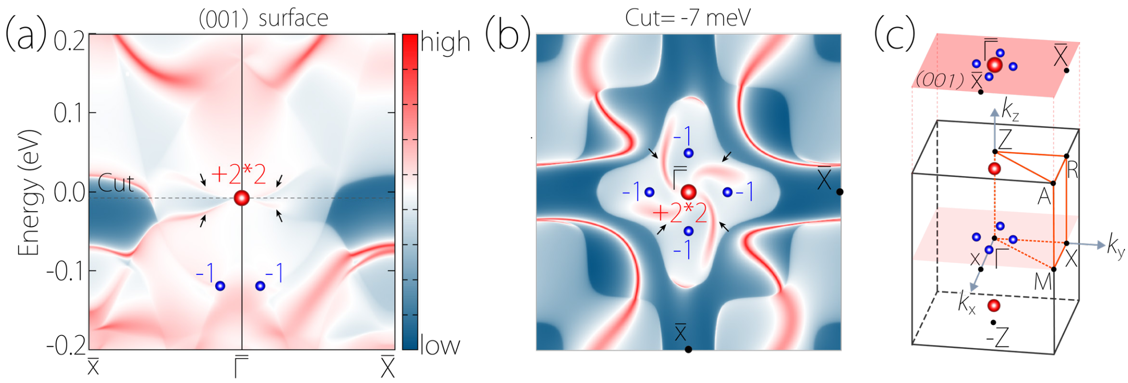

Supplementary Figure S3 | Quadruple spiral Fermi arcs on the (001) surface. a, Calculated surface spectral function projected onto the (001) surface of *r*-THRLN-C_{32} under a -7 GPa hydrostatic pressure. The dashed line indicates the energy level of the constant-energy contour shown in (b). **b**, Isoenergy contour at -7 meV, revealing striking quadruple spiral Fermi arcs connecting the projected topological nodes (indicated by black arrows). **c**, Spatial distribution of the six WPs in the BZ and their corresponding (001) surface projections.

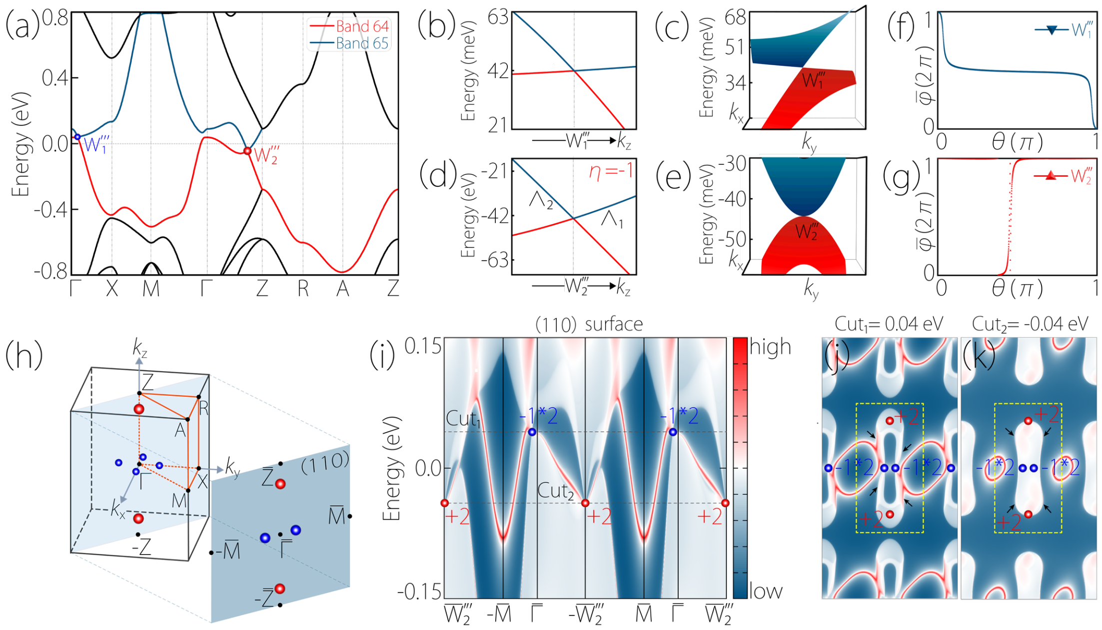

Supplementary Figure S4 | Topological phase transition into two TTWCs under a +6% uniaxial strain along the *c*-axis. Electronic and topological properties of *r*-THRLN-C_{32}. **a**, Bulk band structure along high-symmetry paths showing the formation of W_1''' and W_2''' nodes. **b**, **c**, Linear dispersion profiles of W_1''' across three momentum directions. **d**, **e**, Linear-quadratic mixed dispersion of W_2''', with the IRRs (Λ_1, Λ_2) and the $\eta = -1$ eigenvalue ratio explicitly labeled. **f**, **g**, WCC evolution confirming topological charges of -1 and +2 for W_1''' and W_2''', respectively. **h**, Spatial distribution of the WPs in the BZ and their corresponding (110) surface projections. **i**, Surface spectral function calculated on the (110) boundary. **j**, **k**, Isoenergy contours at 0.04 eV and -0.04 eV, respectively, illustrating the evolution of the Fermi arcs connecting the dissociated TTWCs. Yellow dashed lines denote the first BZ boundaries, and black arrows indicate Fermi arc positions.

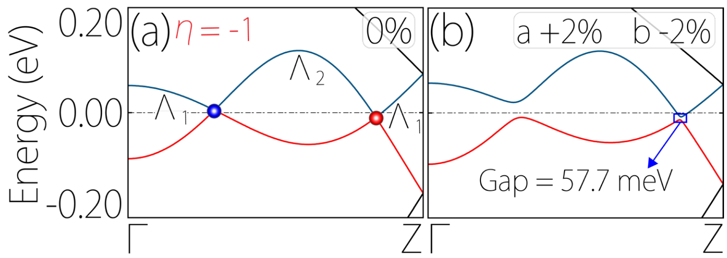

Supplementary Figure S5 | Band structure evolution under asymmetric biaxial strain. a, Schematic of the electronic band evolution for *r*-THRLN-C_{32} subjected to a simultaneous +2% tensile strain along the *a*-axis and a -2% compressive strain along the *b*-axis. The explicit breaking of C_4 symmetry drives a topological phase transition from the pristine phase containing four DWPs ($|C| = 2$, 0% strain) to a conventional WSM phase hosting four pairs of conventional WPs (+2% *a*-axis and -2% *b*-axis).

Table SI. | Space groups and crystallographic parameters for *l*-THRLN-C_{32} and *r*-THRLN-C_{32}. Comparison of the space groups, optimized lattice parameters, and detailed Wyckoff positions for the *l*-THRLN-C_{32} and *r*-THRLN-C_{32} enantiomers.

Structures	Space groups	Lattice parameters (Å)			Wyckoff positions
		a	b	c	
l-CNTFX-C_{32}	$P4_322$	7.32	7.32	5.00	8d (0.43312, 0.29592, 0.37717) 8d (0.54531, 0.30456, 0.12074) 8d (0.91155, 0.58443, 0.31423) 4a (0, 0.2861, 0) 4a (0, 0.91063, 0.5)
r-CNTFX-C_{32}	$P4_122$				8d (0.56688, 0.70408, 0.62283) 8d (0.45469, 0.69544, 0.87926) 8d (0.08845, 0.41557, 0.68577) 4a (0, 0.71391, 0) 4a (0, 0.08937, 0.5)

Table SII. | Elastic constants and corresponding stability criteria for *l*-THRLN-C_{32} and *r*-THRLN-C_{32}.

Structures	Elasticity constants						Stability criteria
	C_{11}	C_{12}	C_{13}	C_{33}	C_{44}	C_{66}	
l-CNTFX-C_{32}	284.129	94.187	107.244	515.490	64.112	3.775	$C_{11} > \|C_{12}\|$; $C_{33} (C_{11}+C_{12}) > 2C_{13}^2$; $C_{44} > 0$; $C_{66} > 0$
r-CNTFX-C_{32}	281.273	94.780	108.679	515.577	64.698	4.199	

Table SIII. | Structural and physical properties of carbon allotropes. Comparison of the space groups, optimized lattice parameters (Å), bond lengths (Å), densities (g/cm^3), total energies E_{tot} (eV per C atom), bulk moduluses (GPa), and corresponding bulk topological properties (WSM: Weyl semimetal, NLSM: nodal-line semimetal) for *l*/*r*-THRLN-C_{32} and other representative carbon allotropes (T-carbon, oC_{24}, cP-C_{24}, fco-C_6, oP16, and Diamond).

Structure	**Space groups**	**Lattice parameters (Å)**			**Band lengths (Å)**	**Density (g/cm^3)**	**E_{tot} (eV/C)**	**Bulk moduluses (GPa)**	**Properties**
		a	**b**	**c**					
l-CNTFX-C_{32} *r*-CNTFX-C_{32}	$P4_322$ $P4_122$	7.32	7.32	5.00	1.38-1.57	2.38	-8.10	189.2	WSM
T-carbon	$Fd\bar{3}m$	7.52	7.52	7.52	1.42,1.50	1.50	-7.92	155.5	Insulator
oC24	*Cmmm*	13.6	8.87	2.47	1.41-1.52	1.60	-9.01	187.1	NLSM
cP-C_{24}	$P4_132$	5.96	5.96	5.96	1.43, 1.45	2.27	-8.45	243.4	WSM
fco-C_6	$F222$ (D_2^7)	6.84	3.33	8.78	1.41-1.49	2.39	-8.46	270.4	WSM
oP16	*Pcca*	4.65	4.28	5.13	1.35-1.69	3.13	-8.68	336.1	NLSM
Diamond	$Fd\bar{3}m$	3.57	3.57	3.57	1.54	3.50	-9.09	434.9	Insulator

Table SIV. | Evolution of the four double-Weyl points under mechanical strain for *r*-THRLN-C_{32}. Exact momentum-space coordinates (k_1, k_2, k_3), energies relative to E_F, chiral topological charges, and multiplicities of the dynamically reconfigured Weyl points (W_1', W_2'; W_1'', W_2''; W_1''', W_2''') subjected to a -7 GPa hydrostatic pressure, a +6% uniaxial strain along the *c*-axis, and a +2% uniaxial strain along the *a*-axis.

Strain Engineering	Space Group	WP	E (meV)	Coordinate (k_1, k_2, k_3)	Charge	Multiplicity
-7GPa	$P4_122$	W_1'	-117.72	$\pm$(0, 0.075, 0)	-1	4
		W_2'	-7.50	$\pm$(0, 0, 0.440)	+2	2
a +2%	$P4_122$	W_1''	-46.69	$\pm$(0.085, 0, 0.141)	-1	4
		W_2''	-5.46	$\pm$(0, 0.089, 0.426)	+1	4
c +6%	$P4_122$	W_1'''	-43.39	$\pm$(0, 0.075, 0)	-1	4
		W_2'''	41.90	$\pm$(0, 0, 0.365)	+2	2

Table SV. Symmetry-allowed space groups hosting exactly four double-Weyl points (DWPs, C-2) in nonmagnetic crystals. The listed space groups (SGs) accommodate this configuration in both the spinless (without SOC) and spinful (with SOC) limits. HSPs/HSLs denote the high-symmetry points or lines at which one and two DWPs are located. IRRs refer to the irreducible (co)representations of the corresponding little groups associated with the Weyl points.

SG	Generators	HSP/Ls for one C-2 WP (IRRs)	HSP/Ls for two C-2 WPS (IRRs)
Without SOC			
75	$\{C_{4z}^{+}\|000\}$, T	Γ({R_2,R_4}); M {R_2,R_4}); Z ({R_2,R_4}); A ({R_2,R_4})	ΓZ ({R_1},{R_3};{R_2},{R_4}); MA ({R_1},{R_3};{R_2},{R_4})
76	$\{C_{4z}^{+}\|00\frac{1}{4}\}$, T	Γ({R_2,R_4}); M ({R_2,R_4})	ΓZ ({R_1},{R_3};{R_2},{R_4}); MA ({R_1},{R_3};{R_2},{R_4})
77	$\{C_{4z}^{+}\|00\frac{1}{2}\}$, T	Γ({R_2,R_4}); M {R_2,R_4}); Z ({R_2,R_4}); A ({R_2,R_4})	ΓZ ({R_1},{R_3};{R_2},{R_4}); MA ({R_1},{R_3};{R_2},{R_4})
78	$\{C_{4z}^{+}\|00\frac{3}{4}\}$, T	Γ({R_2,R_4}); M ({R_2,R_4})	ΓZ ({R_1},{R_3};{R_2},{R_4}); MA ({R_1},{R_3};{R_2},{R_4})
79	$\{C_{4z}^{+}\|000\}$, T	Γ ({R_2,R_4}); Z ({R_2,R_4})	P ({R_1,R_2}); ΓΛ/ΓZ ({R_1},{R_3};{R_2},{R_4}); ZV ({R_1},{R_3};{R_2},{R_4})
80	$\{C_{4z}^{+}\|\frac{3}{4}\frac{1}{4}\frac{1}{2}\}$, T	Γ({R_2,R_4}); Z ({R_2,R_4})	ΓΛ/ΓZ ({R_1},{R_3};{R_2},{R_4}); ZV ({R_1},{R_3};{R_2},{R_4})
89	$\{C_{4z}^{+}\|000\}$, $\{C_{2x}\|000\}$, T	Γ(R_5); M (R_5); Z (R_5); A (R_5)	ΓZ ({R_1},{R_3};{R_2},{R_4}); MA ({R_1},{R_3};{R_2},{R_4})
90	$\{C_{4z}^{+}\|000\}$, $\{C_{2x}\|\frac{1}{2}\frac{1}{2}0\}$, T	Γ(R_5); Z (R_5)	ΓZ ({R_1},{R_3};{R_2},{R_4})
91	$\{C_{4z}^{+}\|00\frac{1}{4}\}$, $\{C_{2x}\|000\}$, T	Γ(R_5); M (R_5)	ΓZ ({R_1},{R_3};{R_2},{R_4}); MA ({R_1},{R_3};{R_2},{R_4})

SG	Generators	HSP/Ls for one C-2 WP (IRRs)	HSP/Ls for two C-2 WPS (IRRs)
92	$\{C_{4z}^{+}\|00\frac{1}{4}\}$, $\{C_{2x}\|\frac{1}{2}\frac{1}{2}0\}$, T		ΓZ ($\{R_1\},\{R_3\};\{R_2\},\{R_4\}$)
93	$\{C_{4z}^{+}\|00\frac{1}{2}\}$, $\{C_{2x}\|000\}$, T	Γ(R_5); M (R_5); Z (R_5); A (R_5)	ΓZ ($\{R_1\},\{R_3\};\{R_2\},\{R_4\}$); MA ($\{R_1\},\{R_3\};\{R_2\},\{R_4\}$)
94	$\{C_{4z}^{+}\|00\frac{1}{2}\}$, $\{C_{2x}\|\frac{1}{2}\frac{1}{2}0\}$, T	Γ(R_5); Z (R_5)	ΓZ ($\{R_1\},\{R_3\};\{R_2\},\{R_4\}$)
95	$\{C_{4z}^{+}\|00\frac{3}{4}\}$, $\{C_{2x}\|000\}$, T	Γ(R_5); M (R_5)	ΓZ ($\{R_1\},\{R_3\};\{R_2\},\{R_4\}$); MA ($\{R_1\},\{R_3\};\{R_2\},\{R_4\}$)
96	$\{C_{4z}^{+}\|00\frac{3}{4}\}$, $\{C_{2x}\|\frac{1}{2}\frac{1}{2}0\}$, T		ΓZ ($\{R_1\},\{R_3\};\{R_2\},\{R_4\}$)
97	$\{C_{4z}^{+}\|000\}$, $\{C_{2x}\|000\}$, T	Γ(R_5); Z (R_5)	P ($\{R_3,R_4\}$); ΓΛ/ΓZ ($\{R_1\},\{R_3\};\{R_2\},\{R_4\}$); ZV ($\{R_1\},\{R_3\};\{R_2\},\{R_4\}$)
98	$\{C_{4z}^{+}\|\frac{3}{4}\frac{1}{4}\frac{1}{2}\}$, $\{C_{2x}\|0\frac{1}{2}\frac{1}{2}\}$, T	Γ(R_5); Z (R_5)	ΓΛ/ΓZ ($\{R_1\},\{R_3\};\{R_2\},\{R_4\}$); ZV ($\{R_1\},\{R_3\};\{R_2\},\{R_4\}$)
168	$\{C_{6}^{+}\|000\}$, T	Γ($\{R_2,R_6\}$; $\{R_3,R_5\}$); A($\{R_2,R_6\}$; $\{R_3,R_5\}$)	ΓA ($\{R_1\},\{R_3\};\{R_1\},\{R_5\};\{R_2\},\{R_4\}$; $\{R_2\},\{R_6\};\{R_3\},\{R_5\};\{R_4\},\{R_6\}$)
169	$\{C_{6}^{+}\|00\frac{1}{6}\}$, T		ΓA ($\{R_1\},\{R_3\};\{R_1\},\{R_5\};\{R_2\},\{R_4\}$; $\{R_2\},\{R_6\};\{R_3\},\{R_5\};\{R_4\},\{R_6\}$)
170	$\{C_{6}^{+}\|00\frac{5}{6}\}$, T		ΓA ($\{R_1\},\{R_3\};\{R_1\},\{R_5\};\{R_2\},\{R_4\}$; $\{R_2\},\{R_6\};\{R_3\},\{R_5\};\{R_4\},\{R_6\}$)

SG	Generators	HSP/Ls for one C-2 WP (IRRs)	HSP/Ls for two C-2 WPS (IRRs)
171	$\{C_6^+\|00\frac{1}{3}\}$, T	Γ({R2,R6}; {R3,R5}); A({R2,R6}; {R3,R5})	ΓA ({R1},{R3};{R1},{R5};{R2},{R4}; {R2},{R6};{R3},{R5};{R4},{R6})
172	$\{C_6^+\|00\frac{2}{3}\}$, T	Γ({R2,R6}; {R3,R5}); A({R2,R6}; {R3,R5})	ΓA ({R1},{R3};{R1},{R5};{R2},{R4}; {R2},{R6};{R3},{R5};{R4},{R6})
173	$\{C_6^+\|00\frac{1}{2}\}$, T		ΓA ({R1},{R3};{R1},{R5};{R2},{R4}; {R2},{R6};{R3},{R5};{R4},{R6})
177	$\{C_6^+\|000\}$, $\{C_{21}'\|000\}$, T	Γ(R5;R6); A(R5;R6)	ΓA ({R1},{R3};{R1},{R5};{R2},{R4}; {R2},{R6};{R3},{R5};{R4},{R6})
178	$\{C_6^+\|00\frac{1}{6}\}$, $\{C_{21}'\|000\}$, T		ΓA ({R1},{R3};{R1},{R5};{R2},{R4}; {R2},{R6};{R3},{R5};{R4},{R6})
179	$\{C_6^+\|00\frac{5}{6}\}$, $\{C_{21}'\|000\}$, T		ΓA ({R1},{R3};{R1},{R5};{R2},{R4}; {R2},{R6};{R3},{R5};{R4},{R6})
180	$\{C_6^+\|00\frac{1}{3}\}$, $\{C_{21}'\|000\}$, T	Γ(R5;R6); A(R5;R6)	ΓA ({R1},{R3};{R1},{R5};{R2},{R4}; {R2},{R6};{R3},{R5};{R4},{R6})
181	$\{C_6^+\|00\frac{2}{3}\}$, $\{C_{21}'\|000\}$, T	Γ(R5;R6); A(R5;R6)	ΓA ({R1},{R3};{R1},{R5};{R2},{R4}; {R2},{R6};{R3},{R5};{R4},{R6})
182	$\{C_6^+\|00\frac{1}{2}\}$, $\{C_{21}'\|000\}$, T		ΓA ({R1},{R3};{R1},{R5};{R2},{R4}; {R2},{R6};{R3},{R5};{R4},{R6})
With SOC			
75	$\{C_{4z}^+\|000\}$, T		ΓZ ({R2},{R6};{R4},{R8}); MA ({R2},{R6};{R4},{R8})
76	$\{C_{4z}^+\|00\frac{1}{4}\}$, T		ΓZ ({R2},{R6};{R4},{R8}); MA ({R2},{R6};{R4},{R8})

SG	Generators	HSP/Ls for one C-2 WP (IRRs)	HSP/Ls for two C-2 WPS (IRRs)
77	$\{C_{4z}^{+}\|00\frac{1}{2}\}$, T		ΓZ ({R_2},{R_6};{R_4},{R_8}); MA ({R_2},{R_6};{R_4},{R_8})
78	$\{C_{4z}^{+}\|00\frac{3}{4}\}$, T		ΓZ ({R_2},{R_6};{R_4},{R_8}); MA ({R_2},{R_6};{R_4},{R_8})
79	$\{C_{4z}^{+}\|000\}$, T		ΓΛ/ΓZ ({R_2},{R_6};{R_4},{R_8}); ZV ({R_2},{R_6};{R_4},{R_8})
80	$\{C_{4z}^{+}\|\frac{3}{4}\frac{1}{4}\frac{1}{2}\}$, T		P ({R_4,R_4}); ΓΛ/ΓZ ({R_2},{R_6};{R_4},{R_8}); ZV ({R_2},{R_6};{R_4},{R_8})
89	$\{C_{4z}^{+}\|000\}$, $\{C_{2x}\|000\}$, T		ΓZ ({R_2},{R_6};{R_4},{R_8}); MA ({R_2},{R_6};{R_4},{R_8})
90	$\{C_{4z}^{+}\|000\}$, $\{C_{2x}\|\frac{1}{2}\frac{1}{2}0\}$, T		ΓZ ({R_2},{R_6};{R_4},{R_8})
91	$\{C_{4z}^{+}\|00\frac{1}{4}\}$, $\{C_{2x}\|000\}$, T		ΓZ ({R_2},{R_6};{R_4},{R_8}); MA ({R_2},{R_6};{R_4},{R_8})
92	$\{C_{4z}^{+}\|00\frac{1}{4}\}$, $\{C_{2x}\|\frac{1}{2}\frac{1}{2}0\}$, T		ΓZ ({R_2},{R_6};{R_4},{R_8})
93	$\{C_{4z}^{+}\|00\frac{1}{2}\}$, $\{C_{2x}\|000\}$, T		ΓZ ({R_2},{R_6};{R_4},{R_8}); MA ({R_2},{R_6};{R_4},{R_8})
94	$\{C_{4z}^{+}\|00\frac{1}{2}\}$, $\{C_{2x}\|\frac{1}{2}\frac{1}{2}0\}$, T		ΓZ ({R_2},{R_6};{R_4},{R_8})
95	$\{C_{4z}^{+}\|00\frac{3}{4}\}$, $\{C_{2x}\|000\}$, T		ΓZ ({R_2},{R_6};{R_4},{R_8}); MA ({R_2},{R_6};{R_4},{R_8})
96	$\{C_{4z}^{+}\|00\frac{3}{4}\}$,		ΓZ ({R_2},{R_6};{R_4},{R_8})

SG	Generators	HSP/Ls for one C-2 WP (IRRs)	HSP/Ls for two C-2 WPS (IRRs)
	$\{C_{2x}\|\frac{1}{2}\frac{1}{2}0\}$, T		
97	$\{C_{4z}^{+}\|000\}$, $\{C_{2x}\|000\}$, T		ΓΛ/ΓZ ($\{R_2\},\{R_6\};\{R_4\},\{R_8\}$); ZV ($\{R_2\},\{R_6\};\{R_4\},\{R_8\}$)
98	$\{C_{4z}^{+}\|\frac{3}{4}\frac{1}{4}\frac{1}{2}\}$, $\{C_{2x}\|0\frac{1}{2}\frac{1}{2}\}$, T		P ($\{R_1,R_4\}$); ΓΛ/ΓZ ($\{R_2\},\{R_6\};\{R_4\},\{R_8\}$); ZV ($\{R_2\},\{R_6\};\{R_4\},\{R_8\}$)
168	$\{C_6^{+}\|000\}$, T		ΓA ($\{R_2\},\{R_{10}\};\{R_2\},\{R_6\};\{R_4\},\{R_{12}\};\{R_4\},\{R_8\};\{R_6\},\{R_{10}\};\{R_8\},\{R_{12}\}$)
169	$\{C_6^{+}\|00\frac{1}{6}\}$, T		ΓA ($\{R_2\},\{R_{10}\};\{R_2\},\{R_6\};\{R_4\},\{R_{12}\};\{R_4\},\{R_8\};\{R_6\},\{R_{10}\};\{R_8\},\{R_{12}\}$)
170	$\{C_6^{+}\|00\frac{5}{6}\}$, T		ΓA ($\{R_2\},\{R_{10}\};\{R_2\},\{R_6\};\{R_4\},\{R_{12}\};\{R_4\},\{R_8\};\{R_6\},\{R_{10}\};\{R_8\},\{R_{12}\}$)
171	$\{C_6^{+}\|00\frac{1}{3}\}$, T		ΓA ($\{R_2\},\{R_{10}\};\{R_2\},\{R_6\};\{R_4\},\{R_{12}\};\{R_4\},\{R_8\};\{R_6\},\{R_{10}\};\{R_8\},\{R_{12}\}$)
172	$\{C_6^{+}\|00\frac{2}{3}\}$, T		ΓA ($\{R_2\},\{R_{10}\};\{R_2\},\{R_6\};\{R_4\},\{R_{12}\};\{R_4\},\{R_8\};\{R_6\},\{R_{10}\};\{R_8\},\{R_{12}\}$)
173	$\{C_6^{+}\|00\frac{1}{2}\}$, T		ΓA ($\{R_2\},\{R_{10}\};\{R_2\},\{R_6\};\{R_4\},\{R_{12}\};\{R_4\},\{R_8\};\{R_6\},\{R_{10}\};\{R_8\},\{R_{12}\}$)
177	$\{C_6^{+}\|000\}$, $\{C_{21}^{'}\|000\}$, T		ΓA ($\{R_2\},\{R_{10}\};\{R_2\},\{R_6\};\{R_4\},\{R_{12}\};\{R_4\},\{R_8\};\{R_6\},\{R_{10}\};\{R_8\},\{R_{12}\}$)
178	$\{C_6^{+}\|00\frac{1}{6}\}$, $\{C_{21}^{'}\|000\}$, T		ΓA ($\{R_2\},\{R_{10}\};\{R_2\},\{R_6\};\{R_4\},\{R_{12}\};\{R_4\},\{R_8\};\{R_6\},\{R_{10}\};\{R_8\},\{R_{12}\}$)
179	$\{C_6^{+}\|00\frac{5}{6}\}$, $\{C_{21}^{'}\|000\}$, T		ΓA ($\{R_2\},\{R_{10}\};\{R_2\},\{R_6\};\{R_4\},\{R_{12}\};\{R_4\},\{R_8\};\{R_6\},\{R_{10}\};\{R_8\},\{R_{12}\}$)
180	$\{C_6^{+}\|00\frac{1}{3}\}$, $\{C_{21}^{'}\|000\}$,		ΓA ($\{R_2\},\{R_{10}\};\{R_2\},\{R_6\};\{R_4\},\{R_{12}\};\{R_4\},\{R_8\};\{R_6\},\{R_{10}\};\{R_8\},\{R_{12}\}$)

SG	Generators	HSP/Ls for one C-2 WP (IRRs)	HSP/Ls for two C-2 WPS (IRRs)
	T		
181	$\{C_6^+ \| 00\frac{2}{3}\}$, $\{C_{21}^{'} \| 000\}$, T		ΓA ($\{R_2\}$,$\{R_{10}\}$;$\{R_2\}$,$\{R_6\}$;$\{R_4\}$,$\{R_{12}\}$; $\{R_4\}$,$\{R_8\}$;$\{R_6\}$,$\{R_{10}\}$;$\{R_8\}$,$\{R_{12}\}$)
182	$\{C_6^+ \| 00\frac{1}{2}\}$, $\{C_{21}^{'} \| 000\}$, T		ΓA ($\{R_2\}$,$\{R_{10}\}$;$\{R_2\}$,$\{R_6\}$;$\{R_4\}$,$\{R_{12}\}$; $\{R_4\}$,$\{R_8\}$;$\{R_6\}$,$\{R_{10}\}$;$\{R_8\}$,$\{R_{12}\}$)